

Regulating the dopant clustering in LiZnAs-based diluted magnetic semiconductor

Zihang Jia(贾子航), Bo Zhou(周波,), Zhenyi Jiang(姜振益), and Xiaodong Zhang(张小东)

Citation: Chin. Phys. B, 2024, 33 (**5**): 058101. DOI: 10.1088/1674-1056/ad3034
Journal homepage: http://cpb.iphy.ac.cn; http://iopscience.iop.org/cpb

What follows is a list of articles you may be interested in

Activated dissociation of H_2 on the Cu(001) surface: The role of quantum tunneling

Xiaofan Yu(于小凡), Yangwu Tong(童洋武), and Yong Yang(杨勇)
Chin. Phys. B, 2023, 32 (**10**): 108103. DOI: 10.1088/1674-1056/acd2b3

Bottom-up design and assembly with superatomic building blocks

Famin Yu(于法民), Zhonghua Liu(刘中华), Jiarui Li(李佳芮), Wanrong Huang(黄婉蓉), Xinrui Yang(杨欣瑞), and Zhigang Wang(王志刚)
Chin. Phys. B, 2022, 31 (**12**): 128107. DOI: 10.1088/1674-1056/ac9e97

Extraordinary mechanical performance in charged carbyne

Yong-Zhe Guo(郭雍哲), Yong-Heng Wang(汪永珩), Kai Huang(黄凯), Hao Yin(尹颢), and En-Lai Gao(高恩来)
Chin. Phys. B, 2022, 31 (**12**): 128102. DOI: 10.1088/1674-1056/ac7bf8

Stability and optoelectronic property of low-dimensional organic tin bromide perovskites

J H Lei(雷军辉), Q Tang(汤琼), J He(何军), and M Q Cai(蔡孟秋)
Chin. Phys. B, 2021, 30 (**3**): 038102. DOI: 10.1088/1674-1056/abc545

Dependence of mechanical properties on the site occupancy of ternary alloying elements in γ'-Ni_3Al: *Ab initio* description for shear and tensile deformation

Minru Wen(文敏儒), Xing Xie(谢兴), Huafeng Dong(董华锋), Fugen Wu(吴福根), Chong-Yu Wang(王崇愚)
Chin. Phys. B, 2020, 29 (**7**): 078103. DOI: 10.1088/1674-1056/ab8a38

Regulating the dopant clustering in LiZnAs-based diluted magnetic semiconductor

Zihang Jia(贾子航)[1], Bo Zhou(周波)[1,2,†], Zhenyi Jiang(姜振益)[1,2,‡], and Xiaodong Zhang(张小东)[1,2,3,4,§]

[1] *Institute of Modern Physics, Northwest University, Xi'an* 710069, *China*
[2] *Shaanxi Key Laboratory for Theoretical Physics Frontiers, Northwest University, Xi'an* 710069, *China*
[3] *Department of Physics, Chinese University of Hong Kong, Hong Kong SAR, China*
[4] *Beijing Computational Science Research Center, Beijing* 100193, *China*

(Received 9 December 2023; revised manuscript received 17 January 2024; accepted manuscript online 5 March 2024)

Tuning of the magnetic interaction plays the vital role in reducing the clustering of magnetic dopant in diluted magnetic semiconductors (DMS). Due to the not well understood magnetic mechanism and the interplay between different magnetic mechanisms, no efficient and universal tuning strategy is proposed at present. Here, the magnetic interactions and formation energies of isovalent-doped (Mn) and aliovalent (Cr)-doped LiZnAs are studied based on density functional theory (DFT). It is found that the dopant–dopant distance-dependent magnetic interaction is highly sensitive to the carrier concentration and carrier type and can only be explained by the interplay between two magnetic mechanisms, i.e., super-exchange and Zener's p–d exchange model. Thus, the magnetic behavior and clustering of magnetic dopant can be tuned by the interplay between two magnetic mechanisms. The insensitivity of the tuning effect to U parameter suggests that our strategy could be universal to other DMS.

Keywords: diluted magnetic semiconductor, dopant distribution, first-principles calculations

PACS: 81.70.Jb, 75.50.Pp, 63.20.dk **DOI:** 10.1088/1674-1056/ad3034

1. Introduction

Efficient doping for modulating the physical properties of semiconductors is essential for meeting the requirement of specific applications of semiconductors. The distribution of dopants, especially the clustering of dopants, significantly affects the performance of semiconductors.[1–12] Although the clustering of dopant is common in semiconductors, the fundamental understanding of the origin of the clustering and the effective strategy to modulate it is still lacking.

The key to tuning the clustering is the classification of interaction between dopants and the interplay between at least two kinds of interactions. For example, the attractive Coulomb interaction between p-type dopants and n-type dopants in Si nanowires[13] hinders the formation of p–n junction. With introduction of inhomogeneous strain, the n-type dopants and p-type dopants can be well separated due to the repulsive stress effect. In this case, the interplay between Coulomb interaction and stress effect determines the distribution of dopants. Another example is the interplay between stress effect and electric field in organic semiconductors doped by two differently sized p-type dopants.[14] These two interactions and their interplay influence the location of dopants. Diluted magnetic semiconductor (DMS) is also an ideal example to demonstrate the effect of interplay between two interactions on dopant distribution.[15–17]

For DMS, the dopant–dopant interaction usually involves at least two interactions, stress effect, and magnetic interaction. The stress effect is usually in the order of tens of meV without external applied strain. Thus, the stress effect solely does not significantly influence the distribution of dopants. The formation energy originating from magnetism may reach to several hundreds of meV. Thus, the formation energy of different dopant distributions is highly sensitive to the magnetic state of the doped system.

Recently, one of the most important progresses in DMS is the finding of the so-called charge and spin-separated systems.[18,19] The charge and spin-separated systems mean the charge and spin part is provided by different elements. For example, the charge is provided by excess Li while the magnetic moment is provided by Mn in Li(Zn,Mn)As system. This is different from traditional (Ga,Mn)As, in which Mn plays the dual role. In fact, spatially homogeneous ferromagnetism has been experimentally realized in Mn-doped I–II–V compounds.[19,20] It is found that the carrier concentration and the Curie temperature indeed can be tuned by Li concentration. Specifically, the Curie temperature increases to 50 K with 10% excess Li and then decreases with larger Li concentration. This finding stimulated a lot of further studies for Mn doping systems with high Curie temperature.[21–25] At present, the reported highest Curie temperature is 230 K in fine-tuned $(Ba_{1-x},K_x)(Zn_{1-y},Mn_y)_2As_2$.[22]

†Corresponding author. E-mail: zhoubo@nwu.edu.cn
‡Corresponding author. E-mail: jiangzhenyi@nwu.edu.cn
§Corresponding author. E-mail: zhangxiaodong@nwu.edu.cn

© 2024 Chinese Physical Society and IOP Publishing Ltd

As a typical charge and spin-separated DMS, LiZnAs has attracted a lot of attention. The magnetic interaction and Curie temperature have been studied by several groups.[26–29] However, the distribution of dopants is rarely studied. Based on the Korringa–Kohn–Rostoker coherent potential approximation (KKR-CPA) method, Sato *et al.* have investigated the magnetic properties of Mn- and Cr-doped LiZnAs and have found that spinodal decomposition is diminished by the introduction of Li vacancies.[30] Such predictions are partly verified by later experiments.[26] Unfortunately, why and how the clustering is influenced by the carrier doping is not clear.

In order to clarify the microscopic origin of clustering and propose a tuning strategy, there are at least two questions need to be answered: First, how to theoretically describe the stability of different distributions of dopant (e.g. dopant cluster). The first question is easy to answer as formation energy is a reasonable index to describe the stability of dopant distribution. Second, how the formation energy of specific distribution of dopant is influenced by the magnetic state and magnetic interaction.

In this paper, we theoretically studied the relative stability of different dopants. The paper is organized as follows: Firstly, we calculated the single doping case. Secondly, we calculated the carrier-dependent magnetic interaction between dopants and discussed the underlying magnetic magnetisms. Thirdly, we calculated the formation energy of different dopant sampling configurations and its relationship with magnetic interaction. Finally, we proved that the findings are not sensitive to U parameter in LDA+U scheme.

2. Computational methods and details

All calculations are performed using projected augmented-wave method[31] and density functional theory within generalized gradient approximation of Perdew–Burke–Ernzerhof[32] as implemented in VASP code.[33] The Mn- or Cr-doped LiZnAs is simulated by $2\times2\times2$ supercell (96 atoms). All atoms are relaxed with force tolerance of 0.01 eV/Å. A plane-wave cut-off energy of 500 eV was used in all calculations. For Brillouin-zone integration, Monkhorst–Pack k-points grid of $4\times4\times4$ was employed. The strong correlation effect of d orbitals is treated by the LDA+U method.[34] The Hubbard parameter $U = 3.5$ eV and Hund exchange parameter $J = 0.6$ eV are taken as suggested by Ref. [18].

LiZnAs crystallizes in a filled-up zinc blende type of structure ($\overline{F}43m$) with a lattice constant of 5.93 Å. As atom at site 4a (0,0,0); Zn atom at site 4d (3/4, 3/4, 3/4), and Li atom at site 4c (1/4, 1/4, 1/4). As is coordinated by 4 Li and 4 Zn atoms with identical distances of about 2.57 Å. Li is bonded to four equivalent As atoms to form $LiAs_4$ tetrahedra that share corners with four equivalent $ZnAs_4$ tetrahedra.[35]

To simulate the short range and long range magnetisms, we use $2\times2\times2$ supercell with two magnetic dopants substituting two Zn atoms, which corresponding to magnetic dopant concentration of 6.25%. Considering the symmetry of LiZnAs, there are 5 types of in-equivalent configurations, corresponding to first nearest neighbor (1st-NN) configuration to fifth nearest neighbor (5th-NN) configuration. The structures of all configurations are shown in Fig. 1. To estimate the image interaction due to finite supercell size, we also calculated the magnetic interaction and formation energy using $3\times3\times3$ supercell. The results are shown in Fig. S1 of the supplementary information. These results suggest that the long range configuration can be stabilized with a different concentration of magnetic dopants. Still, the acceptor concentration should be properly chosen. In the case of $3\times3\times3$ supercell, we found that the long range magnetism can be significantly stabilized upon the doping of three holes. Therefore, these results suggest that the tuning effect is not due to the finite size effect.

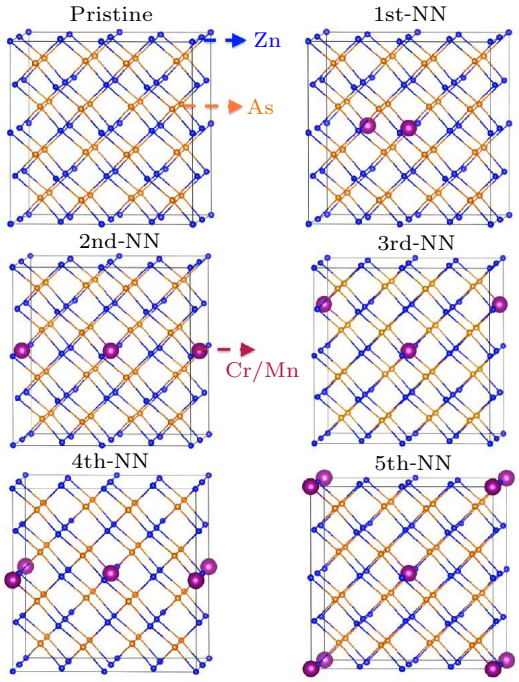


Fig. 1. The crystal structures ($2\times2\times2$ supercell) of pristine and transition metal (Mn and Cr)-doped LiZnAs. The big purple balls are the Mn or Cr atoms, the small blue balls are the Zn atoms, and the small yellow balls are the As atoms. Li atoms are removed for clarity.

As our main focus is the relative stability of different dopant distributions, i.e. clustering or dispersed, the formation energy should be a reasonable index to describe the relative stability. Formation energy of doping system can be well provided by DFT calculations.

The formation energy of transition metal-doped LiZnAs is defined as

$$E_{\mathrm{f}} = E(\mathrm{doped}) - E(\mathrm{undoped}) + n_{\mathrm{Zn}}\mu_{\mathrm{Zn}} - n_{\mathrm{TM}}\mu_{\mathrm{TM}}, \quad (1)$$

where μ_{Zn} and μ_{TM} are chemical potential of Zn and TM, respectively. And n_{Zn} and n_{TM} are numbers of Zn and TM,

respectively. The absolute formation energy is dependent on the choice of chemical potential of Zn and transition metal in our cases. Usually, the chemical potential of Zn or TMs is dependent on the chemical environment, e.g. solid Zn and solid Cr.[26] For theoretical calculations, the total energy of bulk transition metals and Zinc are taken as the chemical potential.[27,29] In fact, the different choices of chemical potential of Zn and TMs do not change our conclusion as these two chemical potentials will be cancelled when comparing formation energy of each configurations.

The predictions based on the formation energy suggest that our results and discussion are at-equilibrium conditions. The missing consideration of entropy (mainly due to the unrealistic computational cost) implies that the conclusions are correct at low temperature. We expect further studies including the entropy term can give more accurate temperature range, in which the conclusions are still valid.

3. Results and discussion

3.1. Single magnetic dopant

In the tetrahedral crystal field, the d orbitals split into lower e_g orbitals and higher t_{2g} orbitals. For pristine LiZnAs, ten d electrons occupy all t_{2g} and e_g orbitals inducing zero magnetic moment. This analysis can be evidenced by the symmetrical density of state (DOS) as shown in Fig. 2(a). As the exchange splitting is large enough as shown in Fig. 2(b),

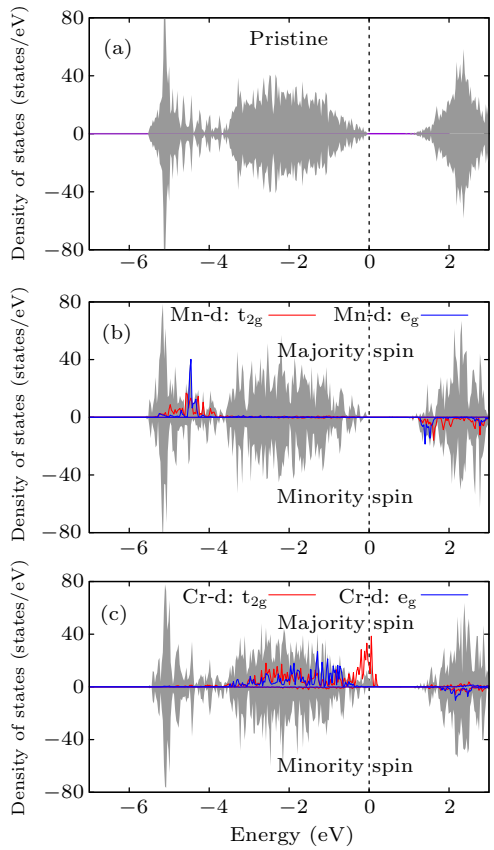


Fig. 2. Density of states of (a) pristine, (b) single Mn-doped, and (c) single Cr-doped LiZnAs.

five electrons of Mn occupy the spin up part of d orbitals. For Cr doping case, two electrons occupy e_g orbitals and two electrons occupy t_{2g} orbital (Fig. 2(c)). Therefore, the magnetic moments should be 5.0 μ_B and 4.0 μ_B for Mn ions and Cr ions, respectively. The calculated magnetic moments of Mn and Cr is 5.0 μ_B and 4.0 μ_B, respectively, which is consistent with the analysis of crystal field splitting. Moreover, the magnetic moment is also consistent with the experimental value of 5.0 μ_B–6.0 μ_B.[19] The above discussion can be clearly evidenced by the anti-symmetric DOS of single Mn- or Cr-doped LiZnAs as shown in Figs. 2(b) and 2(c).

3.2. Hole concentration-dependent magnetic interaction

In order to study the magnetic interaction between two magnetic dopants, we replaced two Zn atoms by two magnetic dopants. The magnetic interaction is defined by the energy difference between anti-ferromagnetic (AFM) and ferromagnetic (FM) states

$$\Delta E = E_{\mathrm{AFM}} - E_{\mathrm{FM}}.$$

It should be noted that this definition is not the routine method evaluating the magnetic interaction, which usually contains the contributions from spin–orbit coupling and magnetic anisotropy. Previous studies and our tests showed that the formation energy is minimally affected by spin–orbit coupling and magnetic anisotropy. Thus, only collinear magnetic coupling is considered here. Such a consideration can ensure the accuracy of formation energy, but cannot give accurate magnetic interaction and other magnetic properties.

According to Zener's model, the magnetic interaction is proportional to the concentration of holes in DMS. The magnetic interaction reaches maximum at proper concentration of holes. In order to find the proper concentration of holes, we calculated the magnetic interaction of 1st-NN under different hole concentrations and the results are shown in Fig. 3.

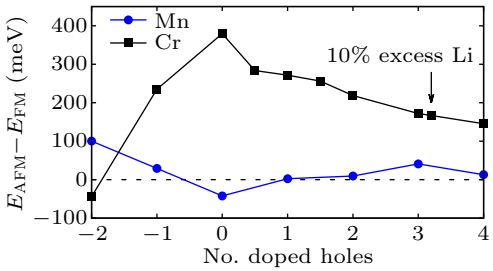


Fig. 3. Hole concentration-dependent magnetic interaction of 1st-NN. Positive value in the horizontal coordinates means the number of holes, negative value means the number of electrons. The magnetic interaction shown here is for 2×2×2 supercell.

For Mn doping case, ferromagnetism is only found in carrier doping case. This is consistent with the experimental finding of Ref. [19] that ferromagnetism is realized in p-type doping case. The magnetic interaction of n-type doping case is larger than that of p-type doping case. This is because the added electron localized around Mn atoms while added holes

prefer delocalized distribution as shown in Figs. S2 and S3 of the supplementary information. The larger concentration of carriers in n-type doping case near Mn atoms leads to much larger magnetic interaction. The electronic phase separation in n-type doping case stabilizes the Mn–As clusters, and hinders the realization of homogeneous DMS. For p-type doping condition, the magnetic interaction reaches maximum at 3.0 holes and then decreases with hole concentration. This result is consistent with the experimental finding that the Curie temperature increases and then decreases with the Li concentration. Such a small magnetic interaction suggests that the room temperature is difficult to realize in p-type LiZnAs.

For Cr-doping case, FM state is the ground state for both intrinsic case and hole doping case. This result is contradict with previous theoretical predictions that anti-ferromagnetic state is stable in Li(Zn,Cr)As case and ferromagnetic phase becomes stable only with excess Li doping case.[27] Later, the authors gave a very different result in their second similar paper.[29] As both references did not consider the correlation effect in their calculations, we also performed the calculations without the consideration of LDA+U scheme. The results also proved that the ferromagnetic state is the ground state. Therefore, the prediction of anti-ferromagnetic state in Ref. [27] could be wrong. We also found that the magnetic interaction reaches its maximum for stoichiometric Li(Zn,Cr)As case. This result suggests that excess Li in Cr-doped $Li_{1+x}ZnAs$ suppresses the magnetic interaction and thus reduces the Curie temperature. Considering the large Curie temperature of 218 K in $Li_{1.1}$(Zn,Cr)As systems,[20] much larger Curie temperature in Li(Zn,Cr)As can be expected with fine tune of the Li concentration.

3.3. Magnetic mechanism

The magnetic mechanism plays the vital role in analyzing the magnetic interaction. For DMS, the contributions of Zener's p–d exchange, super-exchange, and double exchange to magnetic interactions are dependent on the electronic structures of the studied materials.[36] The difference of Zener's model and double exchange lies on the relative position of p levels and d levels. If the p levels are deep-lying and d levels locate in band gap, the double exchange dominates. If the p levels are high and the d levels are relatively lower in energy, the Zener's model dominates. Another difference is that Zener's model is long ranged and can be tuned by carrier concentration while the double exchange is strong and short ranged.

Super-exchange is usually regarded as short ranged and prefers anti-ferromagnetism. However, several studies have found that the super-exchange mechanism can lead to long range ferromagnetism[37] and long range anti-ferromagnetism.[38] The main characteristic is that the super-exchange does not reply on the presence of carriers.

For Mn doping case, super-exchange plays the dominate role in intrinsic case as no carriers exist. When carriers are introduced, the Zener's p–d model plays the role and determines the magnetic state together with intrinsic super-exchange mechanism.[17] The Zener's model can be clearly evidenced by the long range magnetic interaction, which is absent for double exchange. The same magnetic moments of two Mn ions also support the above conclusions.

For Cr doping case, double exchange is not the underlying mechanism because of two facts: the same value of magnetic moments and rather long range nature of the magnetic interactions. These two facts are ignored in previous papers and the double exchange is regarded as the dominant mechanism.[29,30] It is more appropriate to describe the magnetic interaction as the interplay between the super-exchange and Zener's p–d exchange models. The reason is that the Cr^{2+} ion has four electrons occupying d orbitals while the Mn^{2+} ion has five electrons occupying d orbitals. Thus, Cr ions can be regarded as p-type-doped Mn ions. According to the analysis of the Mn doping case, the Cr doping case can be approximately described by super-exchange and Zener's p–d exchange models. Such simplified model can be verified by electron-doped Li(Zn,Cr)As systems as shown in Fig. 3. It is found that 1st-NN prefers AFM with 1 electron/Cr as predicted by above analyses. Moreover, the trend of magnetic interaction of all configurations are also similar to Mn doping case with 1 electron/Cr introduced.

It should be noted that our simple analysis about the magnetic mechanism is also useful for the following analysis based on band coupling model (BCM). The analysis of the exact magnetic mechanism should consider more accurate electronic structure calculations, e.g. DMFT[39] and detailed studies about orbital-resolved magnetic mechanism.[40] These topics are interesting and deserve further effort of the community to clarify the exact mechanism.

3.4. Band coupling model

Based on the understanding of the magnetic mechanisms, we studied the interplay between two magnetic mechanisms and its role to tune the clustering. The interplay between different magnetic mechanisms can be analyzed by BCM. In BCM, the magnetic interactions are described by p–d coupling and d–d coupling. The schematic band BCM diagrams for Cr doping case and Mn doping case are given in Refs. [16,41].

For Mn doping case, majority d states stays below the p states, the energy difference between FM and AFM phases is

$$\Delta_{\mathrm{tot}}^{\mathrm{BCM}} = -m_{\mathrm{h}}(\Delta_{\mathrm{pd}}^{1}+\Delta_{\mathrm{pd}}^{2})+6\Delta_{\mathrm{dd}}^{1,2},\quad 0\le m_{\mathrm{h}}\le 6,$$

where Δ_{pd}^{1} and Δ_{pd}^{2} are p–d coupling strengths for different relative position of t_{2p} level and t_{2d} level. $\Delta_{\mathrm{dd}}^{1,2}$ is the coupling strength between d levels. m_{h} is the number of holes of the

simulating cell. The details of the derivation and the meaning of the parameters can refer to Ref. [16].

For Cr-doping case, majority d states stay above the p states, the energy difference between FM and AFM is given by

$$\Delta_{\rm tot}^{\rm BCM} = \begin{cases} -m_{\rm h}(\Delta_{\rm dd}^{1,2} + \Delta_{\rm dd}^{1}) + 6\Delta_{\rm dd}^{1,2}, & 0 \le m_{\rm h} \le 3, \\ (m_{\rm h} - 3)(\Delta_{\rm dd}^{1} - \Delta_{\rm dd}^{1,2}), & 3 \le m_{\rm h} \le 6. \end{cases}$$

According to BCM, AFM state is more stable than FM state in intrinsic case. With hole doping, FM phase is stabilized. The magnetic interaction increases with the hole concentrations. The maximum of the magnetic interaction is determined by both the types of magnetic dopant and the carrier concentration. These predictions are consistent with DFT results (Fig. 3). Besides, the magnetic interaction is also related to the dopant–dopant distance. For example, the magnetic interaction of 1st-NN is almost zero while the magnetic interaction of other configurations are still finite in proper concentration of carriers. The reason is that the super-exchange and Zener's models have different dependences on distance. As discussed in magnetic mechanism part, the super-exchange decays much faster with distance comparing to Zener's model. Therefore, the long range configurations still have finite magnetic interaction when 1st-NN configuration has almost zero magnetic interaction. Such interplay can be schematically illustrated by Fig. 4. As we all know, the formation energy can be influenced by the magnetic states and magnetic interaction, we expect that the formation energy of different configurations could be tuned by hole concentration. This analysis was verified by the following DFT calculations.

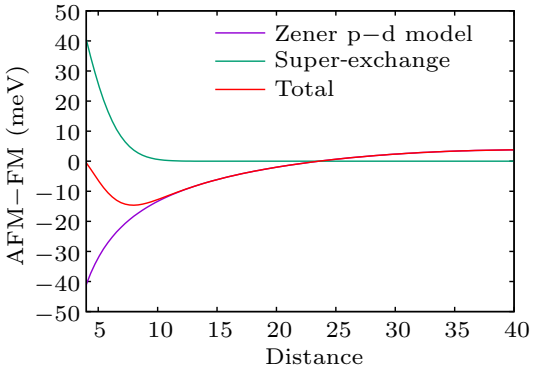


Fig. 4. Schematic picture describing the interplay between super-exchange and Zener's model. The magnetic interaction here is for 2×2×2 supercell.

The predicted hole concentration corresponding to the largest magnetic interaction for BCM and DFT is not precisely consistent. The discrepancy is due to the missing consideration of hole dependence of p–d and d–d coupling strength in BCM.

As the relative p–d and d–d coupling strength is sensitive to concentration of magnetic dopants and pressure, it is expected that the magnetic interaction can be tuned by at least three methods, i.e., carrier concentration, magnetic dopant concentration, and pressure. In fact, such tuning effect is experimentally realized in Ref. [42].

3.5. Relative formation energy and tuning of clustering

Dopant distribution is an important factor of influencing the overall magnetism. Previous analyses of magnetism usually assume the homogeneous distribution of magnetic dopants. However, it is well known that the clustering of magnetic dopants is easy to form and can affect the magnetic properties, e.g. Curie temperature.[43] Thus, it is essential to investigate the tendency of clustering in Cr-doped LiZnAs and give solution to tune it. As explained in Introduction part, the distribution of magnetic dopant is governed by the formation energy. The formation energy determines the relative stability of different dopant samplings. Therefore, we calculated the relative formation energy of Cr doping cases with different carrier concentrations and the results are shown in Fig. 5.

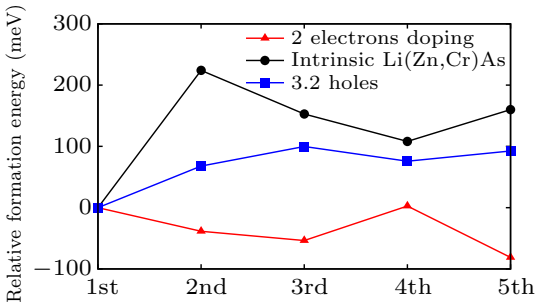


Fig. 5. Relative formation energy of Li(Zn,Cr)As with p-type doping and n-type doping. The formation energy of 1st-NN was set to zero. The formation energy shown here is for 2×2×2 supercell.

We found that the clustering is preferred for intrinsic case and p-type doping case, indicating the clustering is inevitable in those cases. This result is consistent with experimental finding that Cr–As impurity is indeed detected for $Li_{1.1}$(Zn,Cr)As. Interestingly, the clustering can be largely suppressed in n-type doping case. This result is not unexpected as magnetic interaction of 1st-NN is suppressed by electron doping as shown in Fig. 3. The reduced magnetic interaction raises the formation energy of 1st-NN, thus reduces the tendency of clustering. The details of the strategy has also been illustrated by Ref. [17].

Apart from the magnetic interaction, the stress effect also plays some role in determining the relative formation energy. Our tests (unpublished data about isoelectronic doping effect) suggest that the stress energy difference in-between various configurations is up to 10 meV. That means the energy difference arising from the magnetic coupling should be at least larger than 10 meV. This value is not difficult to realize as the typical magnetic interaction (here refer to the energy difference between FM and AFM) is more than 100 meV. So, it is expected that magnetic coupling should be an efficient method to tune the formation energy.

3.6. Influence of U parameters

It is well known that the strong correlation effect of d orbitals has an important influence on magnetic properties. The state-of-art DMFT is an efficient method to treat the strong correlation effect. However, the distance between correlated magnetic ions is usually large (e.g. more than 7 Å) especially in the dilute doping case. In this case, DMFT or cDMFT is difficult to solve such large clusters, which is essential to include the important long range correlation effect between magnetic ions. Therefore, the strong correlation effect was treated by LDA+U scheme in our present studies. The exact value of U parameter is difficult to be estimated although linear response method can self-consistently calculate the value of U. In our studies, we calculated the relative formation energy and magnetic interaction using different U values. If the trend of results is similar with different U settings, our strategy should be still valid. As expected, our results suggested that the trend of relative formation energy and magnetic interaction was not changed with different choices of U parameter (Fig. 6). The different choices of U parameter will influence the critical concentration of carriers corresponding to almost zero magnetic coupling strength, while the trend of reducing the magnetic coupling strength should be similar. Therefore, the strategy to tune the formation energy by the tuning of the magnetic interaction could be applicable to different strong correlation systems (e.g. Cr-doping case and Mn-doping case).

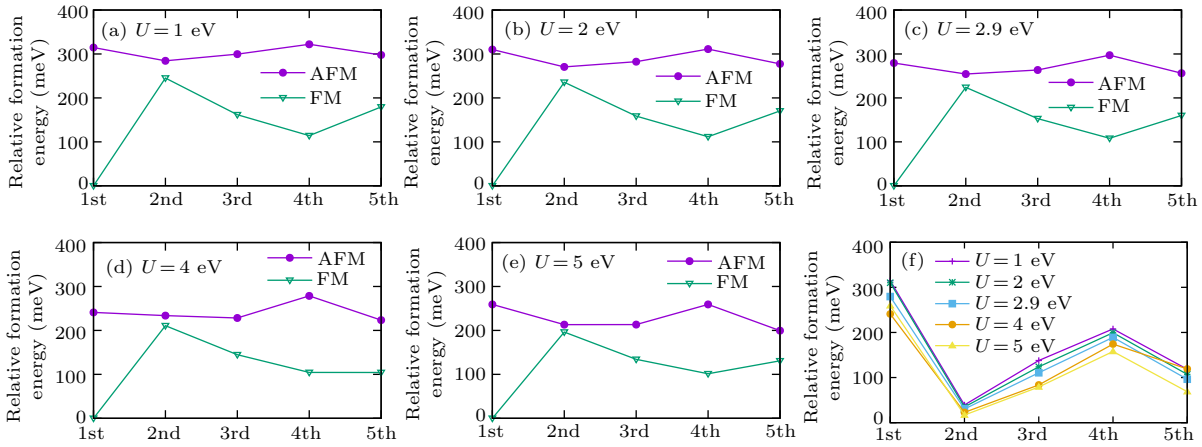


Fig. 6. Relative formation energy and magnetic interaction of Li(Zn,Cr)As with different U parameters. The formation energy of 1st-NN was set to zero. The formation energy here is for 2×2×2 supercell.

Our proposed strategy to tune the clustering relys on the entanglement of two competing magnetic mechanisms, i.e., Zener's model and superexchange. Considering the generality of Zener's model in diluted magnetic semiconductor and the insensitivity of tuning effect to U parameter in the LDA+U scheme, it is expected that such strategy can be applicable to wider range of diluted magnetic semiconductors.

4. Conclusions

Based on the DFT calculations, we investigated the tuning effect of magnetism with carrier concentrations. Based on the analyses of the magnetic mechanism and BCM, the tuning effect of magnetic interaction can be well explained by the interplay between super-exchange and Zener's p–d model. Further, the trend of clustering of magnetic dopants can be explained by such interplay and the results are consistent with the experimental findings. We expect that this tuning strategy can be applied to other DMS.

Acknowledgements

Project supported by the Natural Science Foundation of Shaanxi Province of China (Grant No. 2013JQ1018), the Natural Science Foundation of Department of Education of Shaanxi Province of China (Grant No. 15JK1759) and the Double First-class University Construction Project of Northwest University. The authors are grateful for the financial support of Chinese University of Hong Kong (CUHK) (Grant No. 4053084), University Grants Committee of Hong Kong, China (Grant No. 24300814), and start-up funding of CUHK.

References

[1] Zhao L, He R, Rim K T, Schiros T, Kim K S, Zhou H, Gutirrez C, Chockalingam S P, Arguello C J, Plov L, Nordlund D, Hybertsen M S, Reichman D R, Heinz T F, Kim P, Pinczuk A, Flynn G W and Pasupathy A N 2011 *Science* **333** 999

[2] Aboy M, Santos I, Pelaz L, Marqués L A and López P 2014 *J. Comput. Electron* **13** 40 Elect. 13 40, DOI:

[3] Blavette D and Duguay S 2016 *J. Appl. Phys.* **119** 181502

[4] Boyle C J, Upadhyaya M, Wang P, Renna L A, Lu-Díaz M, Pyo Jeong S, Hight-Huf N, Korugic-Karasz L, Barnes M D, Aksamija Z and Venkataraman D 2019 *Nat. Commun.* **10** 2827

[5] Lin L, Li J, Yuan Q, Li Q, Zhang J, Sun L, Rui D, Chen Z, Jia K, Wang M, Zhang Y, Rummeli M H, Kang N, Xu H Q, Ding F, Peng H and Liu Z 2019 *Sci. Adv.* **5** eaaw8337

[6] Yoshimura A, Koratkar N and Meunier V 2020 *Nano Express* **1** 010008

[7] Chen J, Li J, Sun L, Lin Z, Hu Z, Zhang H, Wu X, Zhang D, Cheng G and Zheng R 2021 *J. Ener. Chem.* **59** 736

[8] Smart T J, Baltazar V U, Chen M, Yao B, Mayford K, Bridges F, Li Y and Ping Y 2021 *Chem. Mater.* **33** 4390

[9] Jang J, Kim J K, Shin J, Kim J, Baek K Y, Park J, Park S, Kim Y D, Parkin S S P, Kang K, Cho K and Lee T 2022 *Sci. Adv.* **8** eabn3181

[10] Hunnestad K A, Hatzoglou C, Khalid Z M, Vullum P E, Yan Z, Bourret E, van Helvoort A T J, Selbach S M and Meier D 2022 *Nat. Commun.* **13** 4783

[11] Goldmann B A, Clarke M J, Dawson J A and Islam M S 2022 *J. Mater. Chem. A* **10** 2249

[12] Lambie S, Steenbergen K G, Gaston N and Paulus B 2022 *Phys. Chem. Chem. Phys.* **24** 98

[13] Zhang D B, Zhao X J, Seifert G, Tse K and Zhu J 2019 *Nat. Sci. Rev.* **6** 532

[14] Mller L, Rhim S Y, Sivanesan V, Wang D, Hietzschold S, Reiser P, Mankel E, Beck S, Barlow S, Marder S R, Pucci A, Kowalsky W and Lovrincic R 2017 *Adv. Mater.* **29** 1701466

[15] Kuroda S, Nishizawa N, Takita K, Mitome M, Bando Y, Osuch K and Dietl T 2007 *Nat. Mater.* **6** 440

[16] Dalpian G M and Wei S H 2006 *Phys. Status Solidi B* **243** 2170

[17] Zhang X, Zhang J, Tse K, Zhang S and Zhu J 2019 *Phys. Rev. B* **99** 134435

[18] Mašek J, Kudrnovský J, Máca F, Gallagher B L, Campion R P, Gregory D H and Jungwirth T 2007 *Phys. Rev. Lett.* **98** 067202

[19] Deng Z, Jin C Q, Liu Q Q, Wang X C, Zhu J L, Feng S M, Chen L C, Yu R C, Arguello C, Goko T, Ning F, Zhang J, Wang Y, Aczel A A, Munsie T, Williams T J, Luke G M, Kakeshita T, Uchida S, Higemoto W, Ito T U, Gu B, Maekawa S, Morris G D and Uemura Y J 2011 *Nat. Commun.* **2** 422

[20] Ning F L, Man H, Gong X, Zhi G, Guo S, Ding C, Wang Q, Goko T, Liu L, Frandsen B A, Uemura Y J, Luetkens H, Morenzoni E, Jin C Q, Munsie T, Luke G M, Wang H and Chen B 2014 *Phys. Rev. B* **90** 085123

[21] Zhao K, Deng Z, Wang X C, Han W, Zhu J L, Li X, Liu Q Q, Yu R C, Goko T, Frandsen B, Liu L, Ning F, Uemura Y J, Dabkowska H, Luke G M, Luetkens H, Morenzoni E, Dunsiger S R, Senyshyn A, Böni P and Jin C Q 2012 *Nat. Commun.* **4** 1442

[22] Zhao K, Chen B, Zhao G, Yuan Z, Liu Q, Deng Z, Zhu J and Jin C 2014 *Chin. Sci. Bull.* **59** 2524

[23] Chen B, Deng Z, Li W, Gao M, Zhao J, Zhao G, Yu S, Wang X, Liu Q and Jin C 2016 *AIP Adv.* **6** 115014

[24] Gu B and Maekawa S 2017 *AIP Adv.* **7** 055805

[25] Guo S, Man H, Wang K, Ding C, Zhao Y, Fu L, Gu Y, Zhi G, Frandsen B A, Cheung S C, Guguchia Z, Yamakawa K, Chen B, Wang H, Deng Z, Jin C Q, Uemura Y J and Ning F 2019 *Phys. Rev. B* **99** 155201

[26] Wang Q, Man H, Ding C, Gong X, Guo S, Jin H, Wang H, Chen B and Ning F L 2014 *J. Appl. Phys.* **115** 083917

[27] Tao H L, Lina L, Zhang Z H, He M and Song B 2016 *Chem. Phys. Lett.* **657** 39

[28] Wang M, Zhang Z, He M, Tao H, Yang T, Song B and Lin L 2017 *J. Super. Nov. Mag.* **30** 1545

[29] Wang M, Tao H, Cui Y, Liu S, He M, Song B, Jian J and Zhang Z 2021 *Chem. Phys. Lett.* **763** 138212

[30] Sato K, Fujimoto S, Fujii H, Fukushima T and Katayama-Yoshida H 2012 *Physica B* **407** 2950

[31] Blöchl P E 1994 *Phys. Rev. B* **50** 17953

[32] Perdew J P, Ruzsinszky A, Csonka G I, Vydrov O A, Scuseria G E, Constantin L A, Zhou X and Burke K 2008 *Phys. Rev. Lett.* **100** 136406

[33] Kresse G and Furthmüller J 1996 *Phys. Rev. B* **54** 11169

[34] Dudarev S L, Botton G A, Savrasov S Y, Humphreys C J and Sutton A P 1998 *Phys. Rev. B* **57** 1505

[35] Hönle W 1993 *Zeitschrift für Naturforschung. B, A J. Chem. Sci.* **48** 683

[36] Sato K, Bergqvist L, Kudrnovský J, Dederichs P H, Eriksson O, Turek I, Sanyal B, Bouzerar G, Katayama-Yoshida H, Dinh V A, Fukushima T, Kizaki H and Zeller R 2010 *Rev. Mod. Phys.* **82** 1633

[37] Chan C, Zhang X, Zhang Y, Tse K, Deng B, Zhang J and Zhu J 2018 *Chin. Phys. Lett.* **35** 017502

[38] Gong W, Leung C H, Sin C K, Zhang J, Zhang X, Xi B and Zhu J 2020 *Chin. Phys. Lett.* **37** 027501

[39] Secchi A, Lichtenstein A and Katsnelson M 2016 *Journal of Magnetism and Magnetic Materials* **400** 112

[40] Kvashnin Y O, Cardias R, Szilva A, Di Marco I, Katsnelson M I, Lichtenstein A I, Nordström L, Klautau A B and Eriksson O 2016 *Phys. Rev. Lett.* **116** 217202

[41] Da Silva J L F, Dalpian G M and Wei S H 2008 *New J. Phys.* **10** 113007

[42] Sun F, Zhao G Q, Escanhoela C A, Chen B J, Kou R H, Wang Y G, Xiao Y M, Chow P, Mao H K, Haskel D, Yang W G and Jin C Q 2017 *Phys. Rev. B* **95** 094412

[43] Dietl T, Sato K, Fukushima T, Bonanni A, Jamet M, Barski A, Kuroda S, Tanaka M, Hai P N and Katayama-Yoshida H 2015 *Rev. Mod. Phys.* **87** 1311